1. POINT-BY-POINT RESPONSE TO REVIEWERS

1.1. Anonymous Referee #1

- R1: “General comments:
This valuable paper presents a well-timed contribution to the current developments in photo-reconstruction and closes a gap for users from various disciplines. As discussed in earlier publications a demand for a straightforward workflow for image based surface reconstruction existed since open source tools (such as vSFM, CloudCompare or meshlab) emerged throughout the last years.
The here presented publication introduces SF3M as a new open source GUI that avoids switching between software including tedious steps of data preparation such as considering different file types for different tools or formatting .asc-files with point cloud data.
The functionality of the tool is achieved by combining the great software CMVS/PMVS (Furukawa and Ponce) respectively the according GUI approach named visualSFM (Wu), various Matlab scripts and point cloud editing tools (filters) from CloudCompare (Girardeau-Montaut).
During this review the program was tested with an own (UAV) datasets. Results proved to be of high quality (dense reconstruction showed very little noise in the point cloud), calculating times were fast and the process all in all stable. In comparison to commercial equivalents the operability can be improved in certain aspects but this also goes along with other open source tools. Final assumptions on the performance of SF3M are not yet to be made as it needs to withstand a trial phase of inexperienced users and different data sets. Nevertheless, first test runs are very promising.
The overall quality of the manuscript is high and with only one exception (description of the “SFM precision”) very comprehensible.

The structure and figures are appropriate. A minor improvement could be achieved by a clear separation of both methods applied: On the one hand the authors present a new approach for data acquisition with a pole and two GoPros and a long walking itinerary while on the other introducing a novel software tool. A clearer distinction between both parts could be given in the introduction. Still, the here described campaign of gully measurement is a good choice to demonstrate the capabilities of the method due to the inherent morphologic complexity of gully systems. As mentioned above, the presented work has the potential to play an important role for DEM generation for non-expert users in various geoscientific contexts.

A1: We will reorganize the introduction to provide a more consistent distinction between the software development (SF3M) and the survey methodology according to the reviewer´s suggestion:

“3D photo-reconstruction (PR) based on structure-from-motion (SfM) algorithms has been applied to date to a large number of geoscience applications (James and Robson, 2012; Westoby et al., 2012; Fonstad et al., 2013). Although there has been a great advance in the last years regarding imagery collection (for instance, derived from the development of UAV platforms) and image processing (commercial as well as free software), the complete photo-reconstruction (PR) and analysis workflow frequently remains lengthy and not straightforward (Kaiser et al., 2014).

If using freely available software, it requires working on a number of different applications to cover basic image pre-processing, photo-reconstruction, georeferencing and post-processing operations. Commercial PR software generally has the ability to perform full PR workflows, but can lack detailed processing information and can restrict user interaction with intermediate and final results. New recent computer developments offer new opportunities to improve data processing. Powerful and freely available

software applications have been developed - e.g. VisualSFM for photo-reconstruction (Wu, 2013) or CloudCompare for cloud processing (Girardeau-Monteaut, 2015) among others - and are being constantly improved through the valuable effort of their developers and users' feedback.

While recent UAV technologies have the capacity of surveying large areas of the landscape (Mathews and Jensen, 2013; Mancini et al., 2013), not all stakeholders (e.g. researchers, technicians and land owners) have the technical and financial resources to use such sophisticated techniques. In addition, government regulations in several countries are becoming increasingly stringent for UAV operations, which hamper the widespread application of this tool. Terrestrial PR approaches represent an alternative which might still be advantageous for several applications, especially when there are regulations or budget constraints as it is frequent in both developing and developed countries. Fonstad et al. (2013) suggested that terrestrial PR techniques could improve their cost-benefit performance by using multiple operators, poles, video capture or a combination of terrestrial and aerial images.

3D PR has been used for gully erosion assessment at the gully reach or headcut scale (Castillo et al., 2012a; Kaiser et al., 2014; Gómez Gutiérrez et al., 2014) and ephemeral gullies (Castillo et al., 2014), usually not more than over a few meters extent. However, the fully characterization of gully erosion requires the assessment of entire gully networks to understand their geometry and dynamics and this brings several challenges for terrestrial PR: 1) morphological complexity: gullies comprise long networks of varying size along their length; 2) valley location: gullies are deep trenches that do not facilitate easy all round image collection, hampering multiple convergent perspectives; 3) linearity: gullies present very high length/width ratios making the photo-reconstruction models more vulnerable to systematic errors.

As an effort to facilitate the use of freely available PR software for demanding gully erosion applications, here we develop a combination of SF3M (a workflow software tool for efficient processing of accurate 3D models of gully networks at a reduced cost) and a rapid terrestrial survey method. For this purpose, 1) we present SF3M, a new graphical user interface to guide PR workflow carried out with existing freely available software; 2) we describe a field methodology for the rapid assessment of gully networks; and 3) we evaluate their performance and the 3D model accuracy with a study case of gully erosion in the Campiña landscape."

- R2: After minor revisions, mainly a few typing errors and suggestions, I fully recommend and support the publication of the manuscript.
Please also note the supplement to this comment:
http://www.soil-discuss.net/2/C161/2015/soild-2-C161-2015-supplement.pdf"

A2: We will answer the reviewer´s comments following this supplement.

- R3 supplement: Page 371, title

I somehow miss the fact that you present a whole new software tool

A3: After the reviewer comment, we have changed the title to: "SF3M software: 3-D photo-reconstruction for non-expert users and its application to a gully network".

- R4 supplement: Page 372, line 3

Alternative: "surface models" as elevation might be misleading to classic DEMs while also pointclouds and meshes are produced

A4: Thank you for the suggestion. We will change to ‘surface models’ in this context.

- R5 supplement: Page 372, line 4

The purpose of this sentence is not clear. Does it refer to challenging scenarios during data acquisition or later data handling?

A5: We will modify the sentence to be more specific: ‘However, innovative approaches are required to overcome some limitations that this technique may present for field image acquisition in challenging scene geometries’.

- R6 supplement: Page 373, line 22

Montaut

A6: Our apologies. This will be corrected in the final version of the manuscript.

- R7 supplement: Page 375, line 17

How was this guaranteed? There might occur an offset during long campaigns due to different exposure times of the GoPro dependent on the lighting. Could this cause issues?

A7: Our apologies. We will change ‘simultaneous’ for ‘near-simultaneous’. It is not necessary for reconstruction purposes in static field scenes to guarantee the exactly synchronised triggering of both cameras. Only a suitable overlap to provide connectivity (image matches) across the image set is required.

- R8 supplement: Page 375, line 17

On

A8: Our apologies. We will correct this in the final version of the manuscript.

- R9 supplement: Page 376, line 7

Could the properties and type of the lens be given?

A9: Our apologies. We will include their specifications in the final version of the manuscript. The first GoPro was modified by installing a 4.14 mm focal length f/3.0 aperture non-fisheye lens and the second one installing a 5.4 mm focal length f/2.8 aperture non-fisheye lens. Both lenses were provided by Peau Productions company (http://peauproductions.com/store/).

- R10 supplement: Page 376, line 14

Information on a potential overlap would be of high interest, especially with regard to the non-fisheye lens.

A10: The camera arrangement (adjacent cameras, that with nadir perspective in a slightly higher position) was designed to provide a very high overlap between images. The nadir camera provides a closer look to the gully while the tilted one captures a larger scene (both in length along the gully and in width across the gully margin). The text will be modified to include a reference to the overlap:

“Both cameras were fixed to the pole end adjacent to each other and held in a horizontal position with the help of plastic wedges and cable ties. One camera looked down in a roughly nadir perspective (closest to the pole end for a higher elevation to compensate for the less deep perspective) and the other was inclined to around 10º. This camera arrangement was intended to: a) obtain a high overlap between images taken with both cameras; 2) ensure the connectivity of the whole image set obtained from different sides of the gully: the two nadir image sets (up- and downwards itineraries) will serve as connectors and the two tilted sets will provide image convergence. Both aspects would be helpful to obtain one single 3-D model with geometric consistency. The typical overlap derived from this camera setting, the walking speed and the time-lapse interval was around 90% for successive images taken from the same camera. As for the overlap between different camera images, the tilted images encompassed totally the scene captured by the nadir camera due to its higher position and inclined orientation”.

- R11 supplement: Page 376, line 21

Please explain the purpose

A11: Using two different colours of GCPs corresponding to odd and even numbers (for instance, for geo-referencing and checking errors respectively) is not really necessary for georeferencing purposes, but it can be useful for deploying the GCPs in the field in an orderly manner. This strategy is advantageous when deploying a GCP on one side of a gully to make easier for the operator to visualize that GCPs are set in alternate positions by looking to the colour of the targets deployed on the other side. Thus, the operator can avoid locating georef or check GCPs on the same area. Ideally, one would prefer to distribute both georeferencing and check points homogenously across the gully. We will modify the text in the following manner:

“Forty five targets, hereafter called ground control points (GCPs), of 20x20 cm dimensions in two colours (pink for even numbers and yellow for odd numbers). This colour symbology was meant to differentiate georeferencing GCPs (even numbers) and error-checking GCPs (odd numbers) to facilitate the operator the deployment of targets in the field.”

- R12 supplement: Page 377, line 1

Maybe a, b, c... would clear things up a bit for the reader as there are two lists with figures entangled.

A12: Our apologies. We´ll follow the reviewer´s suggestion and use letters to order the first list: “a) pre-processing to prepare the image set (automated); b) project definition,

to check the image connectivity and the number of subprojects to process (semi-automated); c) photo-reconstruction (automated); d) georeferencing (semi-automated); e) post-processing (semi-automated)."

- R13 supplement: Page 377, line 7

Space.

A13: Our apologies. We´ll insert the missing blank space.

- R14 supplement: Page 378, line 3

Than.

A14: Our apologies. We´ll change for 'than'.

- R15 supplement: Page 378, line 21

As a general remark it would be advantageous for users to have the numbering fitted to the actual steps in SF3M (e.g. 4. Photo reconstruction). Maybe the first bullet point can stand alone

A15: Although we agree with the reviewer that it would be advisable to be as consistent as possible in the numbering across the manuscript (text and figures), the classification in 2.3. section (Processing methodology in SF3M) focuses on the key features rather than on the specific commands included in the main window of the interface. We believe that trying to follow the same numeration in this case would result in excessive detail and missing the significant contributions of the SF3M design in this section.

- R16 supplement: Page 380, line 6

Please explain how SF3M tackles double z-values in case of undercuttings in gullies during DEM export

A16: The DEM export tool in SF3M follows the classical 2.5 D raster approach of assigning each cell a unique height value (z). Thus, all the height values of the 3D points (x,y,z) falling inside a particular cell are averaged to give this height mean estimate. Although this is a geometrical simplification (higher for coarser raster cell sizes), for many applications this approach may still be valid depending on the objectives of the study. If the user is interested in dealing with full 3D information, the better option would be processing the dense point clouds provided by the photo-reconstruction algorithm directly with a suitable point-cloud processing tool such us CloudCompare.

- R17 supplement: Page 380, line 12

Hard to understand the described procedure, please explain "image measurement".

A17: We have reworded to clarify and to remove the phrase 'image measurement':

"For each point, the local uncertainty is approximated by considering (a) the camera's focal length, (b) the camera-to-point distance in world coordinates, and (c) the maximum image error, where image error is defined as the image distance between an identified feature position and the projection of the associated 3D point in that image."

- R18 supplement: Page 381, line 7

Image collection, GCP deployment...

A18. Our apologies. We will modify the text to clarify the sentence:

"Image collection and GCP operations (deployment and measurement) had similar time requirements, ~90 min each."

- R19 supplement: Page 382, line 25

Include "were"?

A19: Our apologies. We will modify the text to clarify the sentence:

"The points filtered as this last type of vegetation amounted to 4.1% of the total, although its detrimental effects on the model were significant at some gully bottom areas (Fig. 6b)."

- R20 supplement: Page 382, line 27

Bottom.

A20: We´ll correct this. This is included in the former correction.

- R21 supplement: Page 385, line 17

Single heavy rainfall events would be of interest.

A21: Following the reviewer´s suggestion, we will provide some extra information:

"Most likely, the peak of gully erosion took place during the 2009 and 2010, a wet period with annual rainfalls exceeding 1000 mm in the area (425 mm in one month during December 2009-january 2010 and 350 mm during December 2010). These wet years were preceded and followed by seasons closer to the average (650 mm per year)."

- R22 supplement: Page 386, line 7

Besides an evaluation a short outlook would be good: other possible applications, practicable improvements...

A22: Thank you for the suggestion. As an outlook, we will include:

"Therefore, the survey design and processing methodology included in this study is a promising tool for gully erosion evaluation in scenarios with demanding budget and time constraints and reduced operator expertise. Moreover, SF3M provides a means

for easy and fast 3-D photo-reconstruction in other geomorphological applications beyond gully erosion assessment. Future versions of SF3M will try to include new tools including improved GCPs detection and post-processing algorithms such as topographic analysis of the resulting DEM along with further improvement on the interface usability or on other aspects that might be suggested from users´ feedback ".

- R23 supplement: Page 386, line 13

Their

A23: Our apologies. We will correct this in the final version of the manuscript.

- R24 supplement: Page 390, Table 2

Please insert lines above and below (compare to other work steps and required time)

A24: Our apologies. We will correct this in the final version of the manuscript.

- R25 supplement: Page 394, Figure 3

The difference in their angles is hardly visible in this figure.

A25: Yes. This image was included to illustrate the camera settings on the pole (camera positions, wedges and cable ties) rather than differences in angle. We believe that this perspective provides the most practical visual information for other users interested in the image capture procedure. Moreover, a clearly visible depiction of the difference in angle between both cameras is provided schematically in Figure 3c.

1.2. Anonymous Referee #2

- Specific comments

R1: I do not fully understand the automatic discarding and the discarding of blurry images. According to Figure 4, the order is: 3. Reduce number of images, 4. Identify (and discard?) blurry pictures, 6. Undistort pictures. According to Table 2: If 6550 images are taken and 3275 of them are automatically discarded (3275 remain), afterwards 180 blurry images are discarded (3095 remain?), why are 3275 images distorted? If I got it right, this number is wrong.

A1: Our apologies. We will modify the term 'Identify' inside the chart in Figure 4 for 'Discard' to be consistent with the text and the interface tool names. The reviewer is right also in relation with the number of undistorted pictures. We will correct this: 3095 images undistorted (from a total of 6550, we reduced to half -3275- and later 180 were discarded as blurry images → 3095).

R2: I miss additional information concerning the blur metric: Only a footnote in table 1 specifies the metric. The paper defining the metric should be cited (P. Marziliano, F.

Dufaux, S. Winkler and T. Ebrahimi, "'Perceptual blur and ringing metrics: application to JPEG2000"', Signal Processing: Image Communication, vol. 19, no. 2, pp. 163-172, February 2004) and I would like to know, why especially this metric has been chosen. There are plenty of others . . . e. g. compared in Ferzli & Karam: A No-Reference Objective Image Sharpness Metric Based on the Notion of Just Noticeable Blur (JNB). IEEE Transactions on image processing. Vol. 18, No. 4, 2009.

A2: We appreciate the suggestion. The reason behind choosing this specific metric was that a Matlab script by Naccari (2011) was already available which made easier to be integrated inside the SF3M Matlab code. We will include the reference to the Marziliano paper.

R3: Processing times in Table 2 and section 3.2: It is not possible to rate the times without any information concerning the used computer. Especially the search for similar features in pairs is highly parallelizable. Thus, at least the number of cores should be given.

A3: Our apologies. We will include this information in the final manuscript:
“The gully network was processed as three different PR projects (reflecting the number of gully branches) which were then merged in a single point cloud. For the computer used in this study (intel Core i7 2Ghz with 4 cores, 8GB RAM), a total of 2,960 minutes were necessary to process the entire gully network, i.e. ~ 49 hours, of which 17% required operator assistance and 83% only computer time. Photo-reconstruction (54.5% of the total time) and picture undistortion (15.2 %) were the two most time-consuming stages.”

R4: VisualSfM is mainly controlled by an ini-file. Does SF3M change specific settings in this file, e. g. while using Calibration Toolbox? If SF3M changes the file: Are the remaining settings taken from a SF3M source or is only the relevant setting changed in the file?

A4: SF3M modifies automatically the VisualSFM nv.ini settings according to the user´s following choices in the SF3M settings:
1. Maximum number of features (param_gpu_match_fmax in nv.ini file) for the project connectivity analysis. In this case, SF3M modifies this parameter before performing the project connectivity and, once finished, restores the former value (8192 features) into the nv.ini file.

2. The dense reconstruction level and maximum number of images in pmvs2 (param_pmvs_level and param_cmvs_max_image in the nv.ini file) in dense reconstruction.

The rest of the VisualSFM nv.ini parameters are not modified. Regarding the Calibration Toolbox (by Jean Bouguet), this feature is not integrated in SF3M. What our tool includes is the possibility of undistorting the images automatically if the Calib_Results file resulting from the previous tool is available in the project folder.

- Technical corrections:
R5: P. 278, l. 2-3, sentence: "'This list includes generally much fewer image pairs that all the possible combinations among the pictures."' that = than?

A5: Our apologies. We will correct this in the final version of the manuscript.

R6: Figure 4: Two numerations are included in the screenshot: panels (with numbers followed by points) and the relevant graphical control elements (without points).
The reader might be confused, as the numbers in the workflow diagram refer to graphical control elements, though points are used in the diagram.

A6: Our apologies. We will remove the points in the diagram to facilitate the interpretation in the final version of the manuscript. We will also change the Arabic number for the Panel stages on the main window for roman numbers (e.g. 1. Settings to I. Settings).

- Comments concerning the software
This section is intended as remarks for V2.0 of SF3M. From my point of view, they do not (necessarily) need to be considered in the present article.

R7: Assuming my interpretation in the first point of the specific comments is correct:
At first, every n-th image is discarded to reach the percentage given by user in panel 2. Image pre-processing. Afterwards, the blurry images are discarded.
Does this order make sense? Would it not be more reasonable to rate the blurriness at first, discard blurry images and respect the discarded blurry images in the automatic image reducing? Otherwise we might e. g. automatically discard images 2 and 4 due to automatic image reduction, afterwards image 3 because it is blurry. As a consequence, several subsequent images are missing, which might result in an increased dome

effect at this place. If we know that we discard image 3 due to blurriness, it might make sense to keep images 2 and 4!

A7: Thank you for the comment. The Reduce number of images tool was intended to facilitate the user the removal of images following a certain pattern to speed up processing. This is very frequent when taking time-lapse pictures that might result in some cases in an excess of images that would make the process very time–consuming. To us made more sense to reduce first and, once decided the final image set, to proceed with discarding images. Otherwise, this last stage might take a long time since you are working with a much larger dataset. However, reviewer´s suggestion is also feasible by performing the Discard blurry option in the first place (only the non-blurry images will remain in the project folder) and next the Reduce images option (acting on the remaining non-blurry image set).

R8: I would introduce some intelligence in the automatic discarding. The current algorithm assumes truly constant speed of the human taking the images, resulting in a constant overlap of subsequent images. This assumption is at least doubtful and especially not valid for a completely different situation: Let's assume, an UAV is taking the images, traveling at different speeds in different directions due to wind. Thus, it would be more reasonable to rate the overlap (e. b. by simply estimating the spatial autocorrelation (of clipped images)). Then automatically discard e. g. image 2 only if a certain overlap between the images 1 and 3 still is maintained.

A8: Thank you for the suggestion. In fact, a similar approach to that suggested by the reviewer is already working in SF3M. During the project connectivity analysis, SF3M calls VisualSFM for exporting the F-matrix, which only included image pairs with inlier matches. This file is used by SF3M to build the final image pairs file to be used in the photo-reconstruction process. Those pairs with only feature matches not turning to be inliers, are removed from the feature exporting algorithm and, therefore, not processed during the reconstruction stage. This is the main reason why SF3M operation speeds up notably the matching processing by making use of the valuable information provided by the different VisualSFM algorithms.

R9: SF3M uses several freely available third party software like VisualSfM or Cloudcompare. The latter one is being published under GNU General Public License.
In the article, only the description "'freely available"' (p. 374, l. 15) has been used.

Is there any additional comment concerning usage? I did not find any information on the download website, or in the software itself.

A9: Currently, at the http://sf3mapp.csic.es/ website the user can find:
- the Matlab Compiler Runtime
- The SF3M executable and license
- SF3M instructions
- SF3M video tutorials (four videos explaining the complete SF3M workflow).
We will include a brief reference of the information available at the SF3M website in the final version of the manuscript. We have also uploaded the SF3M license to the website. In here we specify that “SF3M is free for personal, non-profit, or academic use. You may redistribute SF3M as long as you make no modifications. Commercial use of this tool is not permited”.

R10: Closely connected to the previous comment: Even slightly deviating workflows will demand modifications in the software. Is there a chance to get the MATLAB files to adapt the user interface to specific workflows?

A10: For a number of reasons, we have decided not to release the source code at this stage. Nevertheless, we actively encourage feedback on the website and will be endeavouring to maintain regular updates to accommodate user requests.

R11: A comment from the software engineer’s point of view: I do not understand, why sometimes checkboxes are used in the GUI (e. g. in panel 2. Image preprocessing), sometimes radio buttons (panel 3., 4. & 5.), although they do not all seem to be arranged in button groups for exclusive selection. It is possible to select several buttons in panel 3. Why?

A11: Thank you for the comment. The Project Panel buttons are not a group. For clarity purposes, they should be modified to check boxes following the reviewer´s suggestion. We will modify this in the final version of the interface and the manuscript.

2. LIST OF RELEVANT CHANGES

- Title: changed to “SF3M software: 3-D photo-reconstruction for non-expert users and its application to a gully network” from answer to Reviewer 1
- Abstract:
    - changed elevation models to ‘surface models’ from answer to Reviewer 1

- sentence reworded to: ‘However, innovative approaches are required to overcome some limitations that this technique may present for field image acquisition in challenging scene geometries’ from answer to Reviewer 1

- Introduction: reorganized from answer to Reviewer 1

- Methodology:

2.1. SF3M: a GUI for efficient photo-reconstruction

- changed ‘Girardeau-Monteaut’ to ‘Girardeau-Montaut’

2.2. Field methodology

- changed ‘simultaneous’ to **‘near-simultaneous’** from answer to Reviewer 1

- changed ‘in’ to **‘on’** from answer to Reviewer 1

- added lenses characteristics ‘In this study, two GoPro Hero3+ cameras equipped with non-fisheye lenses, i.e. 4.14 mm focal length, f/3.0 aperture and 5.4 mm focal length, f/2.8 aperture, respectively (Peau Productions, CA, USA, http://www.peauproductions.com/store/).’ from answer to Reviewer 1.

- added further explanation to camera setting: ‘Both cameras were fixed to the pole end adjacent to each other and held in a horizontal position with the help of plastic wedges and cable ties. One camera looked down in a roughly nadir perspective (closest to the pole end for a higher elevation to compensate for the less deep perspective) and the other was inclined to around 10º. **This camera arrangement was intended to: a) obtain a high overlap between images taken with both cameras; 2) ensure the connectivity of the whole image set obtained from different sides of the gully: the two nadir image sets (up- and downwards itineraries) will serve as connectors and the two tilted sets will provide image convergence. Both aspects would be helpful to obtain one single 3-D model with geometric consistency. The typical overlap derived from this camera setting, the walking speed and the time-lapse interval was around 90% for successive images taken from the same camera. As for the overlap between different camera images, the tilted images encompassed totally the scene captured by the nadir camera due to its higher position and inclined orientation(Fig. 3a and 3b).**’ from answer to Reviewer 1.

- added further explanation to GCPs characteristics: ‘Forty five targets, hereafter called ground control points (GCPs), of 20x20 cm dimensions in two colours (pink for even numbers and yellow for odd numbers). **This colour symbology was meant to differentiate georeferencing GCPs (even numbers) and error-checking GCPs (odd numbers) to facilitate the operator the deployment of targets in the field.**’ from answer to Reviewer 1.

2.3. Processing methodology

- changed numbers to letters: ‘The typical operation for a project reconstruction would include five sequential steps: **a)** pre-processing to prepare the image set (automated); **b)** project definition, to check the image connectivity and the number of subprojects to process (semi-automated); **c)** photo-reconstruction (automated); **d)** georeferencing (semi-automated); **e)** post-processing (semi-automated).’ from answer to Reviewer 1.

- changed ‘that’ to **‘than’** from answer to Reviewer 1.

- added explanation on ‘image measurments’: ‘For each point, the local uncertainty is approximated by considering (a) the camera’s focal length, (b) the camera-to-point distance in world coordinates, and (c) the maximum image error, **where image error is defined as the image distance between an identified feature position and the projection of the associated 3D point in that image**.’ from answer to Reviewer 1.

3. Results

3.1. Field method performance

- sentence reworded to: ‘Image collection and GCP operations (deployment and measurement) had similar time requirements, ~90 min each.’ from answer to Reviewer 1.

3.2. SF3M processing performance

- added further explanation on computer specifications: ‘The gully network was processed as three different PR projects (reflecting the number of gully branches) which were then merged in a single point cloud. For the computer used in this study **(intel Core i7 2Ghz with 4 cores, 8GB RAM)**, a total of 2,960 minutes were necessary to process the entire gully network, i.e. ~ 49 hours, of which 17% required operator assistance and 83% only computer time. Photo-reconstruction (54.5% of the total time) and picture undistortion (15.2 %) were the two most time-consuming stages.’ from answer to Reviewer 1.

- sentence reworded: ‘The points filtered as this last type of vegetation amounted to 4.1% of the total, although its detrimental effects on the model were significant at some gully bottom areas (Fig. 6b).’ from answer to Reviewer 1.

3.4. Gully erosion estimate

- added further information on rainfall characteristics: ‘Most likely, the peak of gully erosion took place during the 2009 and 2010, a wet period with annual rainfalls exceeding 1000 mm in the area **(425 mm in one month during December 2009-january 2010 and 350 mm during December 2010).**’ from answer to Reviewer 1.

4. Conclusions

- added potential future developments on the tool: ‘Therefore, the survey design and processing methodology included in this study is a promising tool for gully erosion evaluation in scenarios with demanding budget and time constraints and reduced operator expertise. **Moreover, SF3M provides a means for easy and fast 3-D photo-reconstruction in other geomorphological applications beyond gully erosion assessment. Future versions of SF3M will try to include new tools including improved GCPs detection and post-processing algorithms such as topographic analysis of the resulting DEM along with further improvement on the interface usability or on other aspects that might be suggested from users´ feedback.**’ from answer to Reviewer 1.

5. Acknowledgements

- changed ‘its’ to ‘their’ from answer to Reviewer 1.

6. References

- changed ‘Girardeau-Monteaut’ to ‘Girardeau-Montaut’ from answer to Reviewer 1.
- reference added ‘Marziliano, P., Dufaux, F., Winkler, S., Ebrahimi, T.: Perceptual blur and ringing metrics: application to JPEG2000. Signal Process.-Image Commun. 19, 163–172. doi:10.1016/j.image.2003.08.003, 2004.’ from answer to Reviewer 2.
- changed ‘Bouguet’ to ’Boughet’.

7. Tables

Table 1:

- added horizontal lines above and below ‘Photo-reconstruction’ from answer to Reviewer 1.
- changed ‘Girardeau-Monteaut’ to ‘Girardeau-Montaut’ from answer to Reviewer 1.
- changed ‘Bouguet’ to ’Boughet’.

- added reference to Marziliano paper: ‘1 Naccari, 2011. Matlab script for image blur metrics based of the blur index developed by Marziliano et al. (2004)’ from answer to Reviewer 2.

Table 2:

- changed number of undistorted pictures: ‘**3095** images undistorted’ from answer to Reviewer 2.

8. Figures

Figure 1:

- changed GUI interface: 1) Arabic number in panels to roman numbers; 2) changed radiobuttons in Project Pannel to check boxes. From answer to Reviewer 2.

-added reference to SF3M license on the website: ‘SF3M executables, license and instructions of SF3M operation can be found in at the SF3Mapp.csic.es domain.’ from answer to Reviewer 2.

Figure 3:

- changed GUI interface: 1) Arabic number in panels to roman numbers; 2) changed radiobuttons in Project Pannel to check boxes. From answer to Reviewer 2.

- Points removed from flow chart on the right side from answer to Reviewer 2.

- changed ‘Identify’ to ‘discard’ in flow chart on the right side from answer to Reviewer 2.

SF3M software: 3-D photo-reconstruction for non-expert users and its application to a gully network~~The SF3M approach to 3D photo-reconstruction for non-expert users: application to a gully network~~

C. Castillo[1,2], M. R. James[3], M. D. Redel-Macías[2] , R. Pérez[2], J. A. Gómez[1].

1 Institute for Sustainable Agriculture. CSIC. Apartado 4084. 14080 Cordoba Spain. *Corresponding author (ccastillo@ias.csic.es)

2 University of Cordoba, Dep. of Rural Engineering, Campus Rabanales, Leonardo Da Vinci Building, 14071 Cordoba, Spain.

3 Lancaster Environment Center. Lancaster University. Lancaster, UK.

Abstract

3D photo-reconstruction (PR) techniques have been successfully used to produce high resolution surface models for different applications and over different spatial scales. However, innovative approaches are required to overcome some limitations that this technique may present for field image acquisition in challenging scene geometries

~~However, innovative approaches are required to overcome some limitations that this technique may present in challenging scenarios~~. Here, we evaluate SF3M, a new graphical user interface for implementing a complete PR workflow based on freely available software (including external calls to VisualSFM and CloudCompare), in combination with a low-cost survey design for the reconstruction of a several-hundred-meters-long gully network. SF3M provided a semi-automated workflow for 3D reconstruction requiring ~49 hours (of which only 17% required operator assistance) for obtaining a final gully network model of >17 million points over a gully plan area of 4,230 m2. We show that a walking itinerary along the gully perimeter using two light-weight automatic cameras (1 second time-lapse mode) and a 6-m-long pole is an efficient method for 3D monitoring of gullies, at a low cost (~1,000 € budget for the field equipment) and time requirements (~90 min for image collection). A mean error of 6.9 cm at the ground control points was found, mainly due to model deformations derived from the linear geometry of the gully and residual errors in camera calibration. The straightforward image collection and processing approach can be of great benefit for non-expert users working on gully erosion assessment. Keywords: Structure-from-motion, gully erosion, photo-reconstruction, accuracy, graphical user interface

1. Introduction

3D photo-reconstruction (PR) based on structure-from-motion (SfM) algorithms has been applied to date to a large number of geoscience applications (James and Robson, 2012; Westoby et al., 2012; Fonstad et al., 2013). Although there has been a great advance in the last years regarding imagery collection (for instance, derived from

the development of UAV platforms) and image processing (commercial as well as free software), the complete photo-reconstruction (PR) and analysis workflow frequently remains lengthy and not straightforward (Kaiser et al., 2014). If using freely available software, it requires working on a number of different applications to cover basic image pre-processing, photo-reconstruction, georeferencing and post-processing operations. Commercial PR software generally has the ability to perform full PR workflows, but can lack detailed processing information and can restrict user interaction with intermediate and final results.

While recent UAV technologies have the capacity of surveying large areas of the landscape (Mathews and Jensen, 2013; Mancini et al., 2013), not all stakeholders (e.g. researchers, technicians and land owners) have the technical and financial resources to use such sophisticated techniques. In addition, government regulations in several countries are becoming increasingly stringent for UAV operations, which hampers the widespread application of this tool.

Thus, there is still a need in developed and developing countries to implement efficient terrestrial PR methodologies (in terms of budget and time requirements) for scientific and technical users concerned with geomorphological processes, such as gully erosion. Fonstad et al. (2013) suggested that terrestrial PR techniques could improve their cost-benefit performance by using multiple operators, poles, video capture or a combination of terrestrial and aerial images. New technologies (such as light-weight cameras) and recent computer developments offer new opportunities to improve data collection and processing. Powerful and freely available software applications have been developed - e.g. VisualSFM for photo-reconstruction (Wu, 2013) or CloudCompare for cloud processing (Girardeau-Monteaut, 2015) among others - and are being constantly improved through the valuable effort of their developers and users' feedback.

3D PR has been used for gully erosion assessment at the gully reach or headcut scale (Castillo et al., 2012a; Kaiser et al., 2014; Gómez Gutiérrez et al., 2014) and ephemeral gullies (Castillo et al., 2014), usually not more than over a few meters extent. However, the fully characterization of gully erosion requires the assessment of entire gully networks to understand their geometry and dynamics and this brings several challenges for terrestrial PR: 1) morphological complexity: gullies comprise long networks of varying size along their length; 2) valley location: gullies are deep trenches that do not facilitate easy all round image collection, hampering multiple convergent perspectives; 3) linearity: gullies present very high length/width ratios making the photo-reconstruction models more vulnerable to systematic errors.

As an effort to facilitate the use of freely available PR software for demanding gully erosion applications, here we develop a combination of a rapid survey method and SF3M, a workflow software tool for efficient processing of accurate 3D models of gully networks at a reduced cost. For this purpose, 1) we present SF3M, a new graphical user interface to guide PR workflow carried out with existing freely available software; 2)

we describe a field methodology for the rapid assessment of gully networks; and 3) we evaluate their performance and the 3D model accuracy with a study case of gully erosion in the Campiña landscape.

2. Material and Methods

2.1. SF3M: a GUI for efficient photo-reconstruction

SF3M v1.0 has been devised as a freely available tool for semi-automated 3D PR to offer a complete workflow from the image set to the 3D model. SF3M v1.0 is written in Matlab® (Mathworks, Natick, MA, USA) and comprises algorithms developed by the authors of this manuscript, a number of previous scripts written by other authors (Table 1) as well as external calls to free software such as VisualSFM (Wu, 2013; Wu, 2015) and CloudCompare (Girardeau-Montaut, 2015). SF3M takes advantage of the command line possibilities already present in these external applications to perform key operations, such as photo-reconstruction (including SIFT features detection, bundle adjustment, sparse and dense reconstruction inside the VisualSFM package) and point cloud processing (i.e. point density, filtering and merging operations in CloudCompare).

The GUI is organized in three windows: main, image and display window (Fig. 1). The main window allows the user to define the operations to be performed. The image window can be used to visualize a photograph, and to enter and delete ground control point (GCP) observations. The display window gives information on the stage in process, time left to finish and main results.

SF3M v1.0 use follows a sequential process including pre-prepocessing, reconstruction, georeferencing and post-processing stages. All the command options are displayed in the main window so that the user can enter the processing options in advance and leave the application running automatically. This design is intended to keep the GUI operation as simple as possible, facilitating its use for non-trained users.

The main features of the SF3M are outlined in Table 1. For a more detailed description of SF3M v1.0 functionalities, the SF3M executable and instructions are available at SF3Mapp.csic.es.

2.2. Field methodology for rapid gully network assessment

We designed a methodology of field image collection for rapid gully erosion reconstruction based on four principles:

1- automated image collection from a pole to capture high centre-perspectives of the gully from its perimeter

2- near-simultaneous capture of two perspectives (two cameras needed oin the pole), with one vertical and the other inclined, to: 1) maximise the probability of

successful image matching between photographs taken from different sides of the gully, in order to achieve a single 3D model; 2) ensure a convergent imaging geometry to help minimise systematic reconstruction errors and model distortion.

3- image capture from only one walking itinerary along the entire gully perimeter

4- use of low-cost devices and materials for image collection

As an application of the SF3M processing method, a gully erosion survey was conducted in a gully network close to the city of Córdoba (Spain) covered with field crops on vertic soils with marls as parent material (37°50'27.4"N, 4°47'59.7"W, Fig. 2). The gully was 510 m long in its main channel and as 11 m wide and 3 m deep in its larger cross sections. Each of the three gully branches were taken as separate photo-reconstruction units in the field and processing stages. The gully network was selected for its convenient location near to Córdoba city as well as for having been filled in during 2008, which provides a baseline to estimate recent gully erosion.

In this study, two GoPro Hero3+ cameras equipped with non-fisheye lenses, i.e. 4.14 mm focal length, f/3.0 aperture and 5.4 mm focal length, f/2.8 aperture, respectively (Peau Productions, CA, USA, http://www.peauproductions.com/store/). The cameras were mounted on a 6 m-long pole (made from a 9 m-long carbon-fibre telescopic fishing rod) to gain height to capture the gully dimensions from a centre position in time lapse capture mode (1 second interval). To reduce camera vibrations, the unused three meters of the telescopic 9-m-long fishing rod were secured with plastic cable ties at the end of the 6 m pole.

Both cameras were fixed to the pole end adjacent to each other and held in a horizontal position with the help of plastic wedges and cable ties. One camera looked down in a roughly nadir perspective (closest to the pole end for a higher elevation to compensate for the less deep perspective) and the other was inclined to around 10º. This camera arrangement was intended to: a) obtain a high overlap between images taken with both cameras; 2) ensure the connectivity of the whole image set obtained from different sides of the gully: the two nadir image sets (up- and downwards itineraries) will serve as connectors and the two tilted sets will provide image convergence. Both aspects would be helpful to obtain one single 3-D model with geometric consistency. The typical overlap derived from this camera setting, the walking speed and the time-lapse interval was around 90% for successive images taken from the same camera. As for the overlap between different camera images, the tilted images encompassed totally the scene captured by the nadir camera due to its higher position and inclined orientation~~Both cameras were fixed to the pole end and held in a horizontal position with the help of plastic wedges and cable ties. One camera looked down in a roughly nadir perspective and the other was inclined to around 10º. This camera arrangement was intended to facilitate the image matching between pictures taken from different sides of the gully along the perimeter itinerary in order to obtain one single 3D model with geometric consistency~~ (Fig. 3a and 3b).

An uninterrupted itinerary along the gully perimeter was followed at a slow walking speed, starting from one point and ending on the opposite side of each gully branch (Fig. 3c). Forty five targets, hereafter called ground control points (GCPs), of 20x20 cm dimensions in two colours (pink for even numbers and yellow for odd numbers). This colour symbology was meant to differentiate georeferencing GCPs (even numbers) and error-checking GCPs (odd numbers) to facilitate the operator the deployment of targets in the field~~Forty five targets, hereafter called ground control points (GCPs), of 20x20 cm dimensions in two colours (pink for even numbers and yellow for odd numbers) were deployed next to the gully edges and at the gully bottom and measured with differential GPS (dGPS, 2 cm accuracy) for georeferencing and error evaluation purposes~~.

2.3. Processing methodology in SF3M

The key features of the processing workflow followed using SF3M v1.0 are listed below:

1. Simplicity in the design and operation, with only one GUI window to define the array of algorithms to run. The typical operation for a project reconstruction would include five sequential steps: a) pre-processing to prepare the image set (automated); b) project definition, to check the image connectivity and the number of subprojects to process (semi-automated); c) photo-reconstruction (automated); d) georeferencing (semi-automated); e) post-processing (semi-automated)~~1) pre-processing to prepare the image set (automated); 2) project definition, to check the image connectivity and the number of subprojects to process (semi-automated); 3) photo-reconstruction (automated); 4) georeferencing (semi-automated); 5) post-processing (semi-automated)~~. Within each of these steps for a PR project, several options can be selected for successive processing, e.g. blurry images detection + image undistortion or green index filter + density filter + Merge + DEM + SfM accuracy. In addition, if the batch mode is activated, the selected operations can be performed over different PR projects.

2. Camera calibration: SF3M does not perform camera calibration. However, SF3M settings include the option to enter camera parameters (focal length and principal point) for use with undistorted images and the fixed camera calibration mode in VisualSFM. In this work, we could not take advantage of this option because VisualSFM does not allow simultaneous use of more than one camera in this mode. Therefore, the internal camera parameters were estimated automatically during the bundle adjustment in VisualSFM.

Furthermore, SF3M allows the user to undistort images if camera calibration data is available from the Matlab Calibration Toolbox (Bouguet, 2014). For our study, both cameras were calibrated using this toolbox and all images were then undistorted keeping the VisualSFM 'determine radial distortion option' disabled.

3. Pair preselection: a first fast run of VisualSFM is performed to identify the significant matches between image pairs (pairs with inlier matches) by comparing all the possible pair combinations, but using only a relatively small number of features from each image for speed. SF3M sets a limit of 1,200 features to use in the VisualSFM settings (the default value is 8,192) for the project connectivity analysis. This value has proved to be sufficiently large to accurately capture the image connection, but at a minimum processing cost.

As a result of this analysis, a list of connected image pairs is generated, which will be the input to the final matching stage. This list includes generally much fewer image pairs thann all the possible combinations among the pictures. The number of the possible combinations (and consequently, processing time) follows a square power law with the number of pictures, while normally the image connection is highly linear (only pictures in the neighbourhood share common features). This results in a significant reduction on the match processing duration, one of the more time consuming stages.

4. Subproject delineation: In SF3M the project connectivity analysis not only checks for the production of a single model and generates an optimal pair list but also provides the approximate locations of cameras with GCPs (provided that GCP observations have been entered by the user in the image window and the search GCPs algorithm performed). This option allows the delineation of subprojects, which are reconstructed separately, by selecting the cameras to be included in the analysis with a polygon drawing tool. Overlapping areas between subprojects are recommended to reduce the errors in the merging process. This tool is advantageous for field surveys where images of the same areas are taken at different times (e.g. in a gully, the upstream and downstream walks on different sides of the same gully region) and to minimise the effects of systematic errors in large image sets.

5. Photo-reconstruction: in SF3M v1.0 the photo-reconstruction stage is carried out through a system call to VisualSFM using command line syntax to drive automated processing. The main VisualSFM commands used in our utility are: extracting SIFT features, image matching, exporting match matrix, bundle adjustment and dense reconstruction (multi-view stereo PMVS2 software, Furukawa and Ponce, 2010).

6. Georeferencing: We followed a similar approach to that developed in SfM_georef (James and Robson, 2012). The GCP observations are entered manually in the image window. The GCP table in the main window provides information on the number of observations per GCP, the image errors (in pixels) and the absolute errors (m). The tool gives the option of selecting which GCP are to be used for georeferencing (georef GCPs) and which other are used to evaluate errors (control GCPs).

7. Dense cloud filtering: SF3M includes two optional filters to be applied to the dense point clouds. The green index filter removes those points with a green index above the threshold selected by the user, for instance, green parts of vegetation standing at the banks or gully bottom. The green index is calculated using GI = 2g-b-r, where r,b an g stands for the pixel value of each of the colour bands in the RGB image (Meyer and

Neto, 2008). The density filter is intended to remove those points with a low point density in their neighbourhood, typically related to lower accuracies. It is also helpful to remove inaccurate points in overlapping areas shared by two dense point clouds which may reduce the accuracy of pre-existent more accurate points. The density filter is performed automatically through command line calls to two CloudCompare algorithms: density calculation and filter by point value.

8. Merging dense point clouds: SF3M automatically merges all the dense point clouds belonging to a subproject using CloudCompare in command line. If subproject definition is not carried out, the resulting merged file is the final dense point cloud. For multiple subprojects, to obtain the final point cloud, the intermediate subproject clouds need to be merged manually by the user (step 9).

9. Point cloud editing: two manual operations were performed fully inside CloudCompare: subproject and project merging, and non-green vegetation filtering.

The merging procedure involves the following algorithms: a) distance cloud-to-cloud of adjacent clouds to determine the specific area inside the overlapping region with minimal errors; b) cropping both point clouds along this area of minimal error to remove the overlapping ; c) merging the point clouds.

To filter non-green vegetation (long-standing greyish prickly weeds, in our case) the point classification algorithm CANUPO (Brodu and Lague, 2012) was used, through its inclusion as a ready-to-use script in CloudCompare. CANUPO performs a point classification into two groups (in this example, weeds and soil) after a training stage carried out by the user.

10. Results: SF3M provides the DEM (average of the z values of points included in a cell of a size defined by the user), a point density map (points/m^2) and an 'SfM precision' map. A decimation factor can be included to speed up the processing, i.e. a factor of ten would include only a tenth of the points in a cell for the computations, for processing large or particularly dense point clouds. We use the term 'SfM precision' to describe local uncertainties in the sparse point cloud. For each point, the local uncertainty is approximated by considering (a) the camera's focal length, (b) the camera-to-point distance in world coordinates, and (c) the maximum image error, where image error is defined as the image distance between an identified feature position and the projection of the associated 3D point in that image~~For each point, the local uncertainty is approximated by considering a) the maximum image error, calculated as the distance between the image measurement and the point projection for the image with the largest error; b) image focal length c) the camera-to-point distance in world coordinates~~. This SfM error is estimated with the following expression:

$$\text{SfM precision (mm)} = \frac{\text{image\_error(pixels)}}{\text{focal\_length(pixels)}} \cdot \text{distance\_point2camera(mm)} \quad [1]$$

Typically, the local precision is higher than the final accuracy measured by ground control reference, since it does not include any wider geometric distortion that may exist across a model. Nevertheless, it provides a useful quantification of photo-reconstruction error on a local basis.

Finally, SF3M v1.0 saves relevant outputs in the main folder for further edition by the user in csv, txt or ascii formats such as matching features, transformation matrices, DEM or point density map, among others. Figure 4 shows the SF3M workflow with indication of the command options to be selected in the main window.

3. Results

3.1. Field method performance

Table 2 shows the field and processing time requirements for this study. A total of 6650 images were taken in the field for the entire gully network at a rate of one picture per second and camera. Approximately 90 min of effective labour (travel to study area, pole preparation and GPS base stationing not considered) were necessary for the field survey. Image collection and GCP operations (deployment and measurement) had similar time requirements, ~90 min each~~Image collection, and GCP deployment and measurement both had similar time requirements, ~90 minutes each~~. Two operators participated in the survey, one for the image capture and the other for GCP measurement, working simultaneously for efficiency purposes.

If no georeferencing had been necessary (for instance, if there is no need of several time series comparison) a much faster approach for scaling and orientation might be followed, using levelled objects of known size, as in previous works (Castillo et al., 2014; Kaiser et al., 2014). In highly linear models such as the gully network, simple procedures (e.g. a carefully levelled several-meters-long thin rope commonly used in construction works) are applicable for later scaling and orientation using a point cloud editing software.

Over recently ploughed gully margins, a walking speed of ~1.5 km/h (approximately a third of normal speed) was necessary to avoid undesired movement in the camera and blurred images. Despite the lightness of the selected materials (pole and cameras) a short break in the image collection was made after completing each of the gully branches to avoid operator fatigue. The camera height (~5 m for the inclined 6 m-long pole) was enough to capture the gully dimensions in its larger cross section (11 m). This gully width seems the maximum achievable for the present image collection design.

3.2. SF3M processing performance

With images taken at 1 second intervals, the image set could be reduced by a factor of two due to repetition within the pictures. The remaining 3,275 images were automatically analysed for blur and 180 images with a blur index greater than two standard deviations above the mean value, were discarded (Fig. 5a).

As expected, the project connectivity showed a multiple-matching pattern reflecting the nadir and tilted camera angles and downstream and upstream walking directions (Fig. 5b). The match matrix diagonal corresponds to the connection between consecutive images; additional lines parallel or perpendicular to the diagonal reflect connectivity between upstream and downstream image groups from the same or different cameras.

The gully network was processed as three different PR projects (reflecting the number of gully branches) which were then merged in a single point cloud. For the computer used in this study (intel Core i7 2Ghz with 4 cores, 8GB RAM), a total of 2,960 minutes were necessary to process the entire gully network, i.e. ~ 49 hours, of which 17% required operator assistance and 83% only computer time. Photo-reconstruction (54.5% of the total time) and picture undistortion (15.2 %) were the two most time-consuming stages~~The gully network was processed as three different PR projects (reflecting the number of gully branches) which were then merged in a single point cloud. A total of 2,960 minutes were necessary to process the entire gully network, i.e. ~ 49 hours, of which 17% required operator assistance and 83% only computer time. Photo reconstruction (54.5% of the total time) and picture undistortion (15.2 %) were the more time consuming stages~~.

All the processing steps were performed using SF3M v1.0 except for those specified in the methods section which required point cloud editing in CloudCompare: 1) subproject merging for the chunks reconstructed separately inside a gully branch to reduce model deformation; 2) project merging for the three gully branches; 3) non-green vegetation filter using CANUPO. Regarding the vegetation filtering, firstly the automated green index filter was applied inside SF3M resulting in a 3.5 % of the total points in the model removed corresponding to small green weeds (Fig. 6a). The second main type of vegetation in the gully was a tall-standing greyish weed, which was filtered using CANUPO. The points filtered as this last type of vegetation amounted to 4.1% of the total, although its detrimental effects on the model were significant at some gully bottom areas (Fig. 6b)~~The points classified and removed as this type of vegetation amounted to 4.1 % of the total, although its detrimental effects on the model were significant at some gully bottoms areas (Fig 6b)~~.

The final gully model had >17 million points over a plan area of 4,230 m^2, making a point density average of 4,020 points/m^2 (Fig. 6c), or approximately 1 point every 2 cm^2, which was sufficient for the 3D modelling purposes at this scale. A higher point density (roughly twice the number of points) could have been achieved by selecting the maximum density level in the pmvs2 algorithm at the cost of longer processing time in the dense reconstruction stage (approximately by a factor of 5). In

352 many applications, higher densities might be impractical and not required for DEM
353 construction. The final photo-reconstruction percentage (the cells with elevation values
354 to total cells ratio) for the 0.25 m DEM was 74.25 %, due to the abundant vegetation
355 occlusion at the gully bottom in certain areas.

356

357 **3.3. 3D Model accuracy**

358 For the present application, an average GCP error of 6.9 cm was found (Fig. 7a).
359 The GCP error is defined as the distance in world coordinates between each GCP centre
360 location in the final georeferenced point cloud and the GCP centre coordinates
361 measured by dGPS in the field. When compared with the average local SfM precision
362 value (Eq. 1), the average GCP error was significantly larger, i.e. 6.9 cm against 2.5 cm
363 (Fig. 7b).

364 There are a variety of sources of error as a consequence of the inexpensive and
365 rapid survey methodology selected in this study such as low-quality camera lenses,
366 uncertainty in the internal camera parameters of the GoPro camera models, reduced
367 number of perspectives from images with only two main angles and the low number of
368 pictures per spatial unit. All these factors may contribute to error in the 3D model both
369 on the local scale (i.e. in the form of uncertainties in the point position) and the model
370 scale (geometrical deformations due to systematic errors accumulating over the model
371 extent).

372 The discrepancy between the GCP error and the estimated SfM precision can be
373 explained mainly as the result of the model deformation at the several-tens-of-meter
374 scale, and is likely to reflect residual error in the camera calibrations (James & Robson,
375 2014). This deformation is visualized as an apparent dome effect at both extremes of
376 each dense point cloud, with increasing error for larger distances from the point cloud
377 centroid. Although the image collection was designed to minimise this effect by
378 specifically including inclined images, doming effects remain noticeable.

379 In this study, the most successful strategy to mitigate the model deformation was
380 to divide the photo-reconstruction project in different subprojects for separate
381 reconstruction using the subproject tool in SF3M. The length of each subproject was
382 defined by the condition of including at least 4 GCPs. Since a total of 45 GCPs were
383 deployed in the field, an average length of ~50 m per subproject was obtained. This
384 approach was advantageous in terms of overall accuracy but implied an additional
385 processing time for manually stitching and merging the 17 subprojects in
386 CloudCompare by determining the area of minimal error between adjacent point clouds.

387 If the subproject definition strategy would not be applied, for instance by
388 reconstructing a several-hundred-meters gully reach in one project, the deformation
389 errors would have been in the order of several tens of centimeters. Similarly, James and
390 Robson (2014) found doming deformations of ~0.2 m over horizontal distances of ~100

m for simulations representative of UAV flights. Their recommendations on using fixed calibration to avoid doming errors could not be followed because VisualSFM does not include a fixed calibration option for multiple cameras.

When compared with previous studies on gully erosion assessment through SfM photo-reconstruction (Castillo et al., 2012a; Gómez-Gutiérrez et al., 2014; Kaiser et al., 2014; Castillo et al., 2014) in terms of unitary efficiency (field effort per meter of gully), this work showed larger errors (roughly 2 times the average errors in those studies) but at a lower survey intensity (images per meter of gully) and at one order of magnitude lower time requirements (Table 3).

3.4. Gully erosion estimate

The resulting DEM was used to estimate the gully volume and a gully erosion estimate, taking the 2008 filled situation as a reference. The volume was determined using the Cut and Fill algorithms in ArcGis^{TM} 9.3 (ESRI Inc., Redlands, CA, USA). The gully limits were delineated manually by interpreting the DEM and slope maps since, in some areas, the gully rims were not well represented in the dense point cloud and automated methods were not fully applicable.

A total gully volume of 3,484 m^3 was obtained for a drainage area of 10.9 has at the gully network outlet. We assumed that the gully was filled in the summer of 2008 (common period for this operation in the Campiña landscape) since the orthophotography (april 2009) shows the gully already filled (Fig. 8). Also, due to the similarity in the gully network of 2011 and 2014 (present study), there is no evidence of further major filling operations between these dates.

Considering a bulk soil density of 1.5 Mg/ m^3, typical of vertic soils in our conditions and a time span of six years, an average gully erosion estimate of 79.5 Mg/ha·year was calculated. Most likely, the peak of gully erosion took place during the 2009 and 2010, a wet period with annual rainfalls exceeding 1000 mm in the area (425 mm in one month during December 2009-january 2010 and 350 mm during December 2010). These wet years were preceded and followed by seasons closer to the average (650 mm per year)~~Most likely, the peak of gully erosion took place during the 2009 and 2010, a wet period with annual rainfalls exceeding 1,000 mm in the area preceded and followed by seasons closer to the average (650 mm per year)~~. This high value of mean gully erosion is in agreement with previous assessments for similar conditions over the same period (Castillo et al., 2012b).

4. Conclusions

3D photo-reconstruction techniques based on SfM algorithms have already demonstrated their capability for producing accurate 3D models in a range of

geoscience applications. Nevertheless, research is still needed to improve efficiency in a number of challenging situations and their ease of use for workers not necessarily skilled in photogrammetric applications. SF3M v1.0 proved to be an efficient and flexible tool for 3D photo-reconstruction in these regards, considering its simplicity and complete workflow.

To the author´s knowledge, this is the first time an entire several-hundred-meters-long gully network has been surveyed by terrestrial photo-reconstruction. This was carried out using inexpensive means (around 1,000 € budget for the field equipment), little manpower (a minimum of one operator is required), in a short time span and has achieved moderate accuracies. Therefore, the survey design and processing methodology included in this study is a promising tool for gully erosion evaluation in scenarios with demanding budget and time constraints and reduced operator expertise. Moreover, SF3M provides a means for easy and fast 3-D photo-reconstruction in other geomorphological applications beyond gully erosion assessment. Future versions of SF3M will try to include new tools including improved GCPs detection and post-processing algorithms such as topographic analysis of the resulting DEM along with further improvement on the interface usability or on other aspects that might be suggested from users´ feedback~~Therefore, the survey design and processing methodology included in this study is a promising tool for gully erosion evaluation in scenarios with demanding budget and time constraints and reduced operator expertise~~.

5. Acknowledgements

This study was supported by Projects P08-AGR-03925 (Andalusian Government) and AGL2009-12936-C03-01 (Spanish Ministry of Science and Innovation), AGL2012-40128-C03-01 (Spanish Ministry of Economy and Competitiveness), RESEL (Spanish Ministry for Environment and Rural and Marine Affairs) and FEDER funds. This support is gratefully acknowledged. The authors would like to thank José Manuel Cabezas for his contribution in the gully survey. We also express our gratitude to all developers of freely available software for ~~its~~ their generous contributions, especially to Changchang Wu and Daniel Girardeau-Montaut.

6. References

Boughuet, J.: Undistortion script (Matlab Camera Calibration Toolbox). http://www.vision.caltech.edu/bouguetj/calib_doc/ (last access December 2014).

Brodu, N., and Lague, D.: Terrestrial lidar data classification of complex natural scenes using a multi-scale dimensionality criteria : applications in geomorphology. Journal of Photogrammetry and Remote Sensing 68: 121-134. (IF 2.90), 2012.

Castillo, C., Pérez, R., James, M.R., Quinton, J.N., Taguas, E.V., and Gómez, J.A.: Comparing the Accuracy of Several Field Methods for Measuring Gully Erosion. Soil Sci. Soc. Am. J. 76, 1319–1332. doi:10.2136/sssaj2011.0390, 2012a.

Castillo, C., Pérez, R., Mora., J., Gómez, J.A.: Quantification of gully erosion in a cultivated area in Southern Spain under high rainfall conditions. Geophysical research abstracts, 14, EGU 2012-10976, 2012b.

Castillo, C., Taguas, E.V., Zarco-Tejada, P., James, M.R., and Gómez, J.A.: The normalized topographic method: an automated procedure for gully mapping using GIS. Earth Surf. Process. Landf. 39, 2002–2015. doi:10.1002/esp.3595, 2014.

Castillo, C., Rodríguez, A., Giráldez, J.V., and J.A. Gómez: Mejora de la evaluación de la erosión por flujo concentrado en taludes de carreteras sobre diferentes materiales en Andalucía mediante foto-reconstrucción., Avances de la geomorfología en España 2012-2014, 176-179, 2014.

Fonstad, M.A., Dietrich, J.T., Courville, B.C., Jensen, J.L., and Carbonneau, P.E.: Topographic structure from motion: a new development in photogrammetric measurement. Earth Surf. Process. Landf. 38, 421–430. doi:10.1002/esp.3366, 2013.

Furukawa, Y., and Ponce, J.: Accurate, dense, and robust multiview stereopsis. IEEE Trans. Pattern Anal. Mach. Intell. 32(8):1362–1376. doi:10.1109/TPAMI.2009.161, 2010.

Girardeau-Monteaut, D.: CloudCompare: 3D point cloud and mesh processing software. http://www.danielgm.net/cc/ (last Access, 20 March 2015).

Gómez-Gutiérrez, A., Schnabel, S., Berenguer-Sempere, F., Lavado-Contador, F., and Rubio-Delgado, J.: Using 3D photo-reconstruction methods to estimate gully headcut erosion. Catena 120, 91–101. doi:10.1016/j.catena.2014.04.004, 2014.

James, M.R., and Robson, S.: Straightforward reconstruction of 3D surfaces and topography with a camera: Accuracy and geoscience application. J. Geophys. Res.-Earth Surf. 117, F03017. doi:10.1029/2011JF002289, 2012.

James, M.R., and Robson, S.: Mitigating systematic error in topographic models derived from UAV and ground-based image networks. Earth Surf. Process. Landf. 39, 1413–1420. doi:10.1002/esp.3609, 2014.

Junta de Andalucía, Consejería de Medio Ambiente y Ordenación del Territorio: http://www.juntadeandalucia.es/medioambiente/site/rediam/menuitem.aedc2250f6db83cf8ca78ca731525ea0/?vgnextoid=0863d61d8470f210VgnVCM2000000624e50aRCRD&lr=lang_es (last access 20 March 2015).

Kaiser, A., Neugirg, F., Rock, G., Mueller, C., Haas, F., Ries, J., and Schmidt, J.: Small-Scale Surface Reconstruction and Volume Calculation of Soil Erosion in Complex Moroccan Gully Morphology Using Structure from Motion. Remote Sensing 6, 7050–7080. doi:10.3390/rs6087050, 2014.

Código de campo cambiado

Mancini, F., Dubbini, M., Gattelli, M., Stecchi, F., Fabbri, S., and Gabbianelli, G.: Using Unmanned Aerial Vehicles (UAV) for High-Resolution Reconstruction of Topography: The Structure from Motion Approach on Coastal Environments. Remote Sens. 5, 6880–6898. doi:10.3390/rs5126880, 2013.

Marziliano, P., Dufaux, F., Winkler, S., Ebrahimi, T.: Perceptual blur and ringing metrics: application to JPEG2000. Signal Process.-Image Commun. 19, 163–172. doi:10.1016/j.image.2003.08.003, 2004.

Mathews, A.J., and Jensen, J.L.R.: Visualizing and Quantifying Vineyard Canopy LAI Using an Unmanned Aerial Vehicle (UAV) Collected High Density Structure from Motion Point Cloud. Remote Sens. 5, 2164–2183. doi:10.3390/rs5052164, 2013.

Meyer, G.E., and Neto, J.C.: Verification of color vegetation indices for automated crop imaging applications. Comput. Electron. Agric. 63, 282–293. doi:10.1016/j.compag.2008.03.009, 2008.

Naccari, M.: Blur_metric script. https://sites.google.com/site/matteonaccari/software, 2011 (last access November 2014).

Stevens, A.: Arcgridwrite matlab script. http://www.mathworks.com/matlabcentral/fileexchange/16176-arcgridwrite/content/arcgridwrite.m, 2007 (last access november 2014).

Westoby, M.J., Brasington, J., Glasser, N.F., Hambrey, M.J., and Reynolds, J.M.: "Structure-from-Motion" photogrammetry: A low-cost, effective tool for geoscience applications. Geomorphology 179, 300–314. doi:10.1016/j.geomorph.2012.08.021, 2012.

Wu, C.: Towards linear-time incremental structure from motion. International Conference on 3D vision publication (3DV Conference, Seattle, WA, USA, June 2013), 127-134, 2013.

Wu, C.: VisualSFM : A Visual Structure from Motion System. http://ccwu.me/vsfm/ , 2015 (last access, 3 March 2015).

Con formato: Inglés (Reino Unido)

Table 1. SF3M v1.0 features showing the aim of each stage, and software used.

SF3M FEATURES	Purpose	External software	
		Tool	Type
Preprocessing			
Reducing the number of pictures	Decrease the total number of images	----	----
Detecting blurry images	Discard blurry images.	Blur_metric[1]	Matlab script
Renaming pictures	Change the initial character string of the image name	----	----
Picture undistortion	Undistortion of pictures	Undistort[2]	Matlab script
Project			
Project connectivity	Check if the image set produces a single model	VisualSFM[3]	3D Photo-reconstruction
Search GCPs in pictures	Identify GCP candidate by colour in images to facilitate GCP observations input	----	----
Preliminary camera location with GCPs	Approximated location of cameras to facilitate subproject definition	----	----
Subproject definition	Generate different separate subsets for PR	----	----
Photo-reconstruction			
Sparse and dense reconstruction	3D model in relative SfM coordinates	VisualSFM[3]	3D Photo-reconstruction
Georeferencing			
GCP observations input and deletion	Managament of GCP observations by visual identification on image window	----	----
Highlight of images with detected GCPs	Facilitates GCP observations input on image window	----	----
Highlight of images with observation and GCP number	Facilitates GCP observations input and removal	----	----
Georef GPC and control GCP	Setting GCP reference and control errors	----	----
Calculation of image errors	Errors in image measurements (collinearity equations)	----	----

Con formato: Inglés (Reino Unido)

Con formato: Inglés (Reino Unido)

Con formato: Inglés (Reino Unido)

Con formato: Inglés (Reino Unido)

Transformation matrix, georef and control errors	Absolute error determination	----	----
Application of transformation matrix for each option file	Transforming the dense point clouds from camera to world coordinates	----	----
Post-processing			
Green index filter	Removing points canditates to vegetation in dense clouds	----	----
Density filter	Removing points with low point density in its neighborhood	CloudCompare[4]	Point cloud editing
Merge dense	Merge dense point clouds for subprojects	CloudCompare[4]	Point cloud editing
Results			
DEM (m)	DEM in asc format as an elevation average in a cell	arcgridwrite[5]	Matlab script
Point density (points/m2)	Point density map	----	----
SfM precision (mm)	SfM error in sparse point cloud (Eq. 1)	----	----

[1] Naccari, 2011. Matlab script for image blur metrics based of the blur index developed by Marziliano et al. (2004); [2]Boughuet, 2014; [3]Wu, 2013; [4]Girardeau-Monteaut, 2015; [5]Stevens, 2007

Con formato: Justificado

569 Table 2. Field and processing time requirements for the entire gully network. Main
570 results and type of operation are included.

SF3M operation	Operation	Result	Time (min)
Field survey			**170**
Image collection	Manual	6550 images	80
GCP deployment and GCP measurement	Manual	45 GCPs measured	90
Preprocessing			**487**
Reducing the number of pictures	Automated	3275 images discarded	5
Detecting blurry images (blur index threshold = 2)	Automated	180 images discarded	32
Picture undistortion	Automated	~~3275~~ 3095 images undistorted	450
Project analysis			**263**
Project connectivity	Automated	Matrix of matches	55
Search GCPs in pictures	Automated	GCP identified in image window	48
Manual input GCP observations	Manual	300 observations from 45 GCP	120
Manual subproject delineation	Manual	17 subprojects	40
Photo-reconstruction			**1,615**
Sparse reconstruction	Automated	17 sparse clouds	765
Dense reconstruction (medium level)	Automated	119 dense files	850
Georeferencing			**60**
Calculation of image errors	Automated	Image errors	--
Calculation of transformation matrix, georef and control errors	Automated	Georef errors	--
Application of transformation matrix for each option file	Automated	119 georeferred dense clouds	60
Post-processing			**318**

Green index filter (green index threshold = 30)	Automated	Average of 3.5 % points removed	68
Density filter	Automated	Average of 1.2 % points removed	55
Merge dense clouds	Automated	17 merged clouds	25
Merge subprojects and projects	Manual	1 final point cloud	110
Remove non-green vegetation (Canupo)	Manual	Average of 4.1 % points removed	60
Results			**47**
DEM (m) and Point density (points/m2)	Automated	DEM and point density ascii file	25
SfM precision (mm)	Automated	SfM accuracy map for a project	22
			2,960

571

572

573

574 Table 3. Comparison between the survey intensity (number of pictures per meter of
575 gully) and time requirements (image collection time per meter of gully) for different
576 gully erosion studies using SfM photo-reconstruction including the present study.

577

Author	Year	Gully feature	Length (m)	Average Errors (m)	Number of pictures	Time for image collection (min)	Survey intensity (pictures/m)	Time requirements (min/m)
Castillo et al.	2012a	Reach	7.1	0.025	191	10	26.9	1.4
Gómez-Gutiérrez et al.	2014	Headcut	6	0.048	64	NA	10.7	NA
Kaiser et al.	2014	Headcut	4	--	257	30	64.3	7.5
Castillo et al.	2014	Ephemeral	30	0.036	515	90	17.2	3.0
Present study	**2015**	**Network**	**750**	**0.069**	**3,275**	**80**	**4.4**	**0.1**

578

579

580

581

582

583

584

585

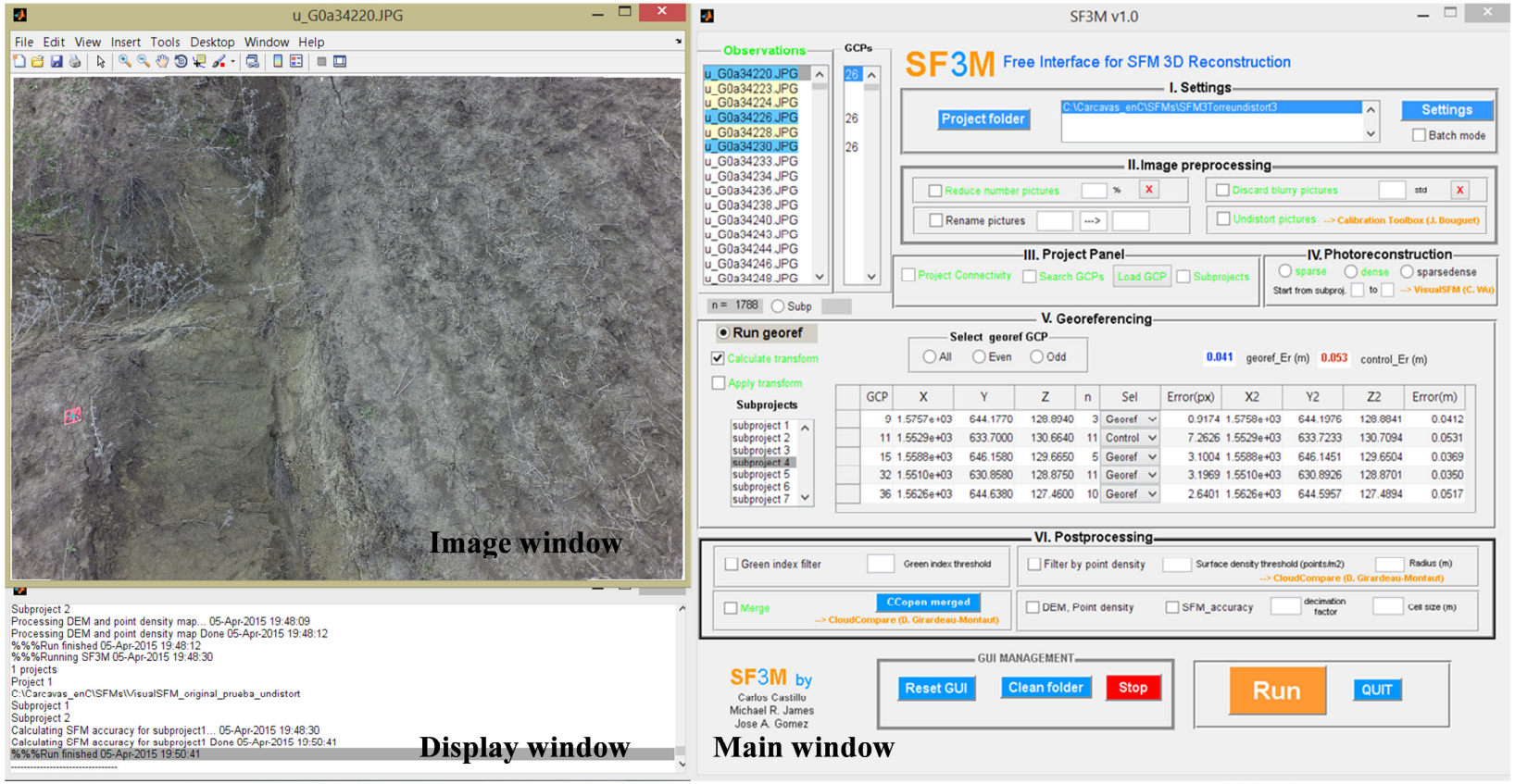
u_G0a34220.JPG
File Edit View Insert Tools Desktop Window Help
Image window
Subproject 2
Processing DEM and point density map... 05-Apr-2015 19:48:09
Processing DEM and point density map Done 05-Apr-2015 19:48:12
%%%Run finished 05-Apr-2015 19:48:12
%%%Running SF3M 05-Apr-2015 19:48:30
1 projects
Project 1
C:\Carcavas_enC\SFMs\VisualSFM_original_prueba_undistort
Subproject 1
Subproject 2
Calculating SFM accuracy for subproject1... 05-Apr-2015 19:48:30
Calculating SFM accuracy for subproject1 Done 05-Apr-2015 19:50:41
%%%Run finished 05-Apr-2015 19:50:41
Display window
SF3M v1.0
Observations
GCPs
SF3M Free Interface for SFM 3D Reconstruction
I. Settings
Project folder
C:\Carcavas_enC\SFMs\SF3M3Torreundistort3
Settings
Batch mode
II. Image preprocessing
Reduce number pictures
Discard blurry pictures
Rename pictures
Undistort pictures --> Calibration Toolbox (J. Bouguet)
III. Project Panel
Project Connectivity
Search GCPs
Load GCP
Subprojects
IV. Photoreconstruction
sparse
dense
sparsedense
Start from subproj.
to
--> VisualSFM (C. Wu)
n = 1788
Subp
V. Georeferencing
Run georef
Calculate transform
Apply transform
Subprojects
subproject 1
subproject 2
subproject 3
subproject 4
subproject 5
subproject 6
subproject 7
Select georef GCP
All
Even
Odd
0.041 georef_Er (m)
0.053 control_Er (m)
GCP X Y Z n Sel Error(px) X2 Y2 Z2 Error(m)
9 1.5757e+03 644.1770 128.8940 3 Georef 0.9174 1.5758e+03 644.1976 128.8841 0.0412
11 1.5529e+03 633.7000 130.6640 11 Control 7.2626 1.5529e+03 633.7233 130.7094 0.0531
15 1.5588e+03 646.1580 129.6650 5 Georef 3.1004 1.5588e+03 646.1451 129.6504 0.0369
32 1.5510e+03 630.8580 128.8750 11 Georef 3.1969 1.5510e+03 630.8926 128.8701 0.0350
36 1.5626e+03 644.6380 127.4600 10 Georef 2.6401 1.5626e+03 644.5957 127.4894 0.0517
VI. Postprocessing
Green index filter
Green index threshold
Filter by point density
Surface density threshold (points/m2)
Radius (m)
--> CloudCompare (D. Girardeau-Montaut)
Merge
CCopen merged
--> CloudCompare (D. Girardeau-Montaut)
DEM, Point density
SFM_accuracy
decimation factor
Cell size (m)
SF3M by
Carlos Castillo
Michael R. James
Jose A. Gomez
GUI MANAGEMENT
Reset GUI
Clean folder
Stop
Run
QUIT
Main window

586

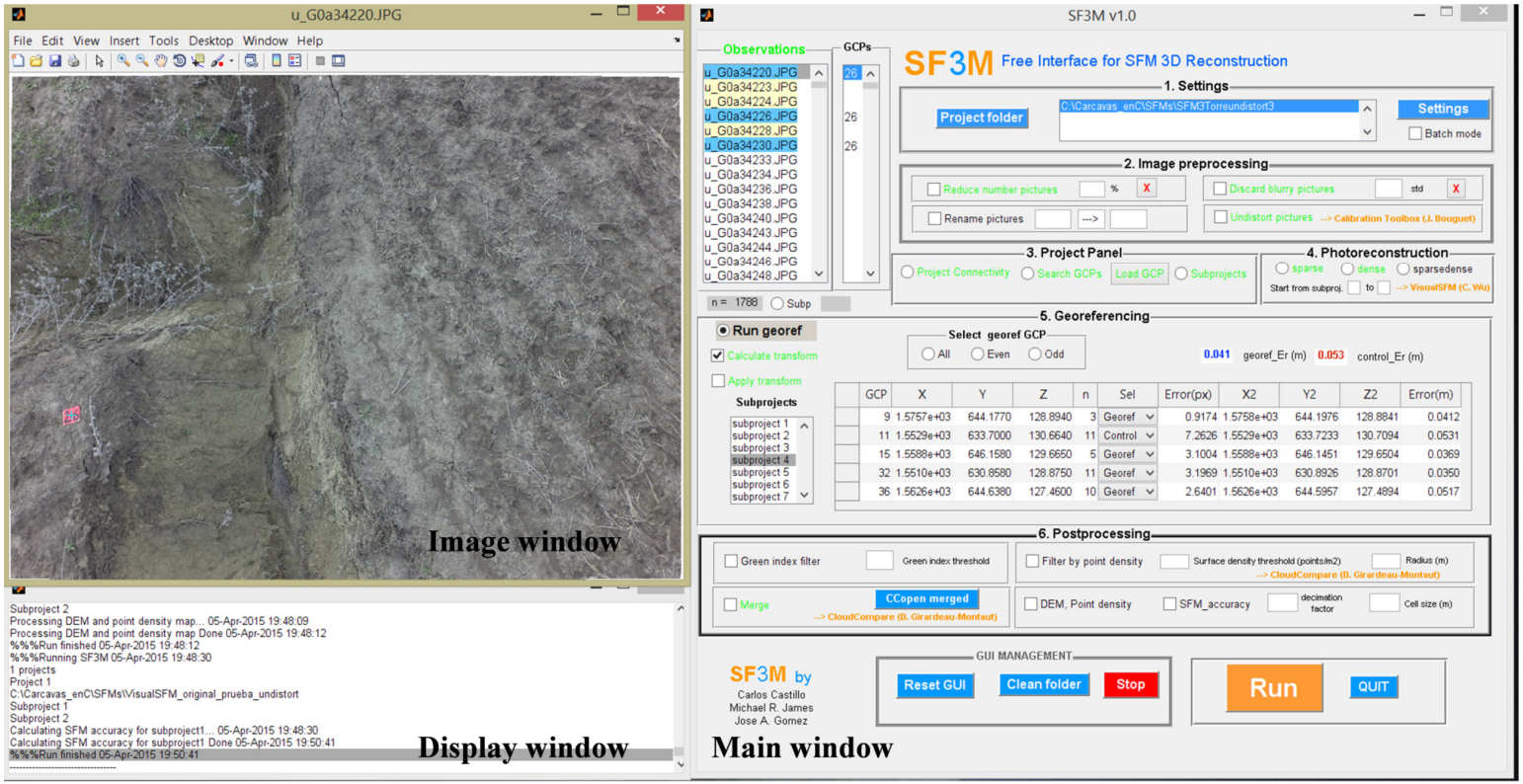

Figure 1. SF3M v1.0 with the main window on the right, image window on the upper-left and display window on the bottom-left. Among other SF3M features, the figure shows: 1) highlighting of image listbox with detected ground control points GCPs (yellow) and with observations (blue) in the observations window; 2) text in green colour for performed operations; 3) subproject listbox for subproject management; 4) GCPs

table with mean georef and control errors. SF3M executables, license and ~~A complete manual~~instructions ~~of SF3M operation~~ can be found ~~in~~ at the SF3Mapp.csic.es domain.

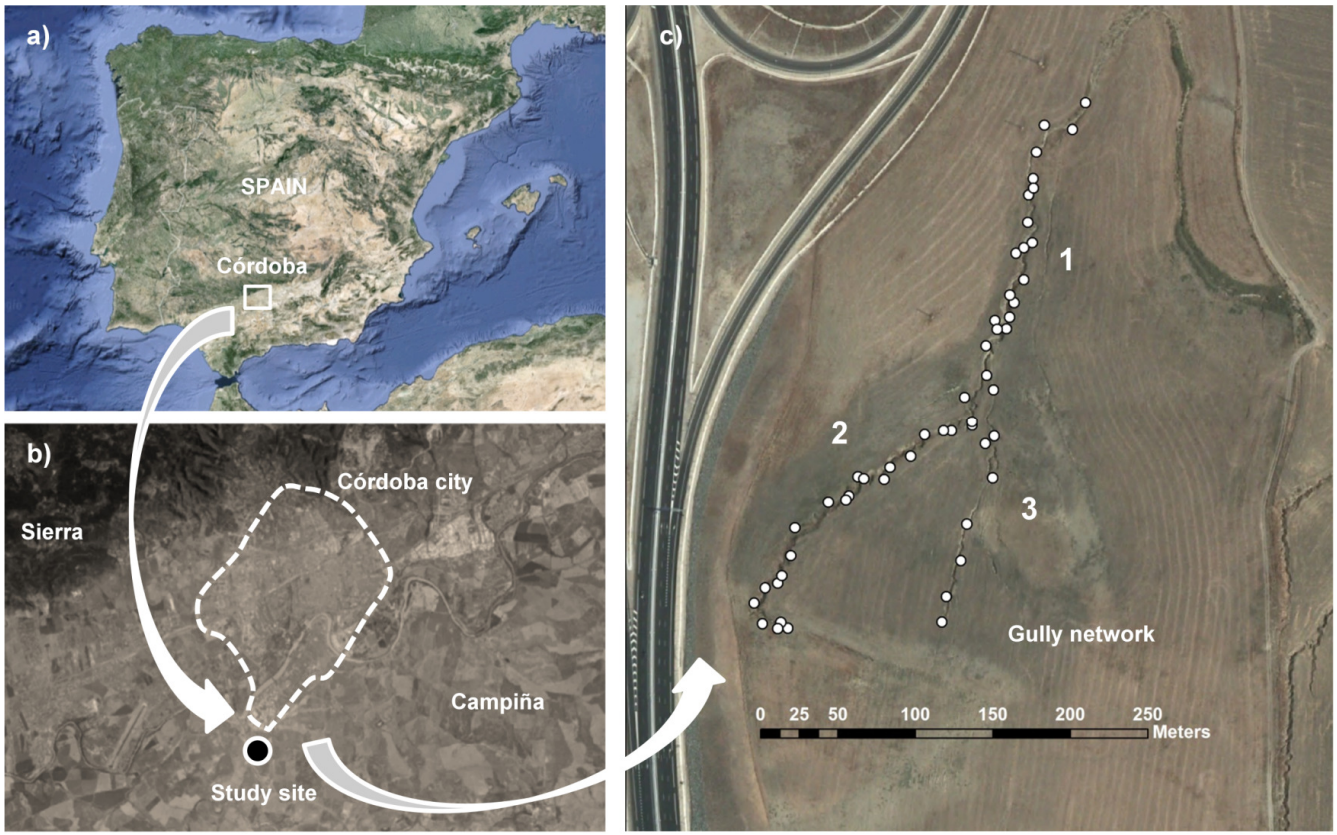

Figure 2. a) and b) Location of the study site (source: https://www.google.es/maps); c) Plan view of the gully network with indication of the branch number for photo-reconstruction purposes from the 2011 orthophotography (Junta de Andalucía, 2015). In white dots, the location of the ground control points GCPs deployed in the gully.

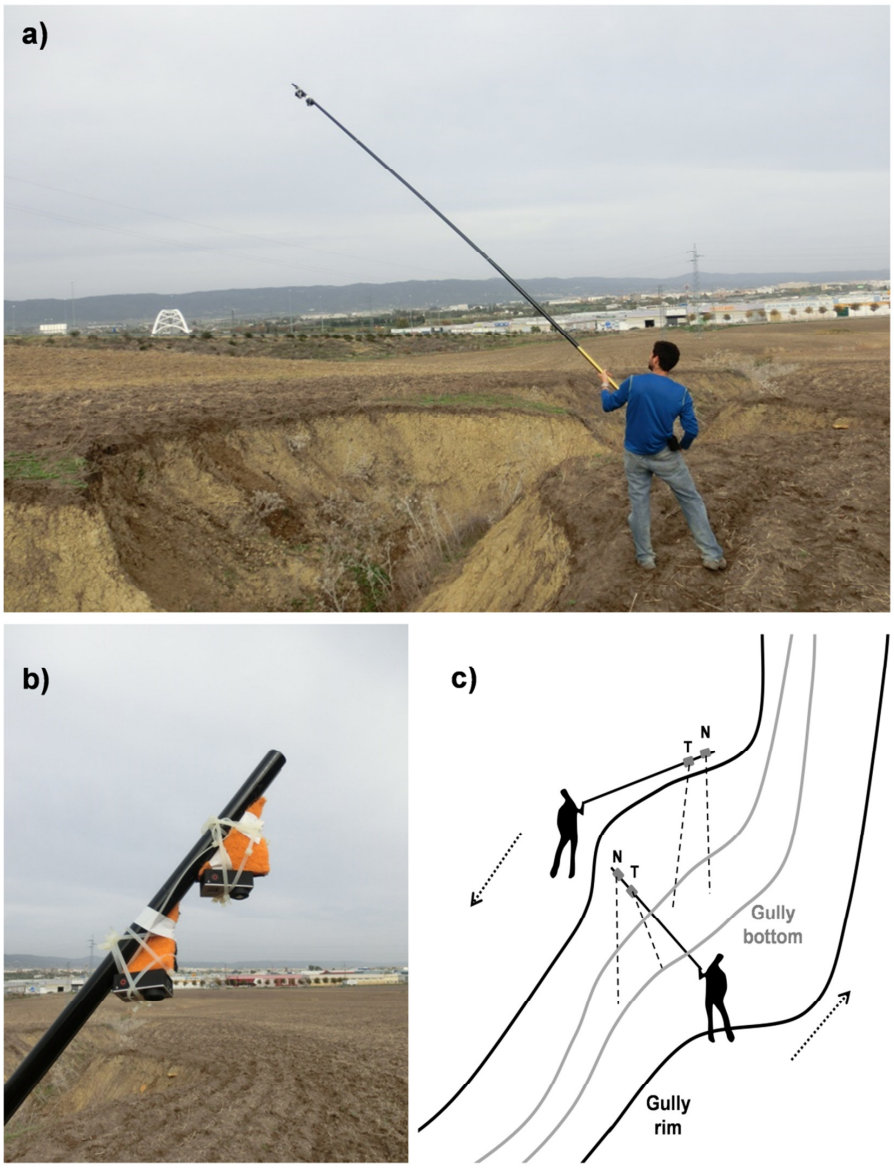

Figure 3. Camera operation in the gully erosion study: a) View of the operator during the field survey; b) Closer view of the two GoPro Hero3+ cameras on the 6 m pole with differential angle between cameras. c) Sketch of the image collection methodology as a walking itinerary along the gully perimeter. The rough nadir perspective (N) corresponds to the camera close to the pole tip and the tilted perspective (T) to the camera slightly below.

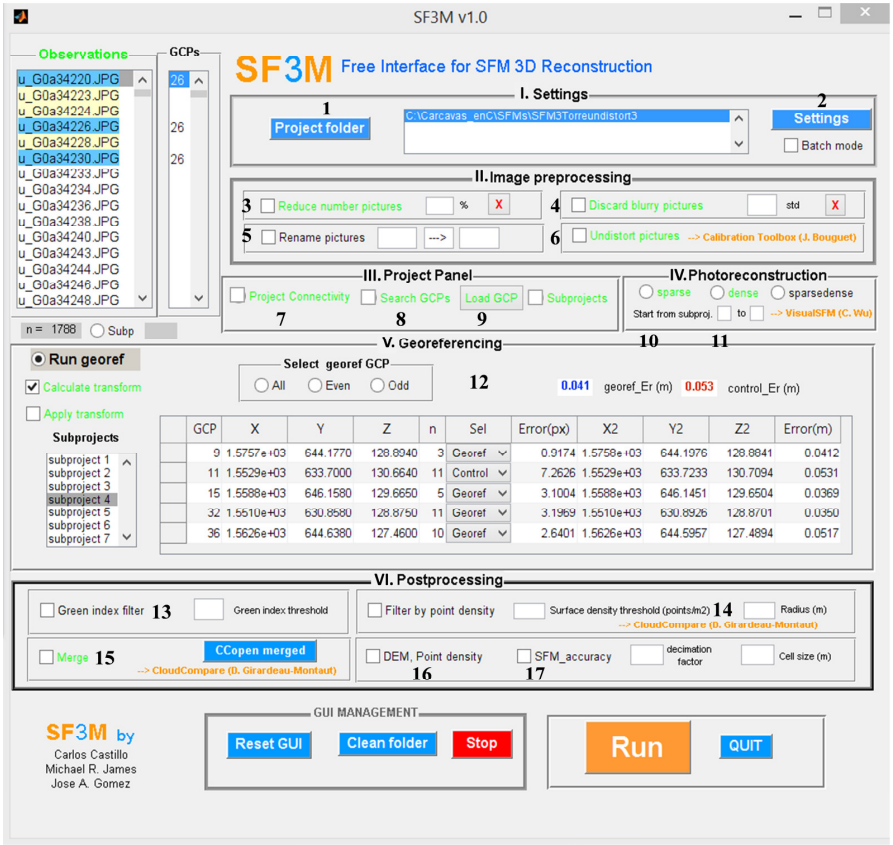
SF3M v1.0
Observations
GCPs
SF3M Free Interface for SFM 3D Reconstruction
I. Settings
Project folder
Settings
Batch mode
II. Image preprocessing
Reduce number pictures
Discard blurry pictures
Rename pictures
Undistort pictures
III. Project Panel
Project Connectivity
Search GCPs
Load GCP
Subprojects
IV. Photoreconstruction
sparse
dense
sparsedense
V. Georeferencing
Run georef
Calculate transform
Apply transform
Select georef GCP
All
Even
Odd
georef_Er (m)
control_Er (m)
Subprojects
VI. Postprocessing
Green index filter
Green index threshold
Filter by point density
Surface density threshold (points/m2)
Radius (m)
Merge
CCopen merged
DEM, Point density
SFM_accuracy
decimation factor
Cell size (m)
SF3M by
Carlos Castillo
Michael R. James
Jose A. Gomez
GUI MANAGEMENT
Reset GUI
Clean folder
Stop
Run
QUIT

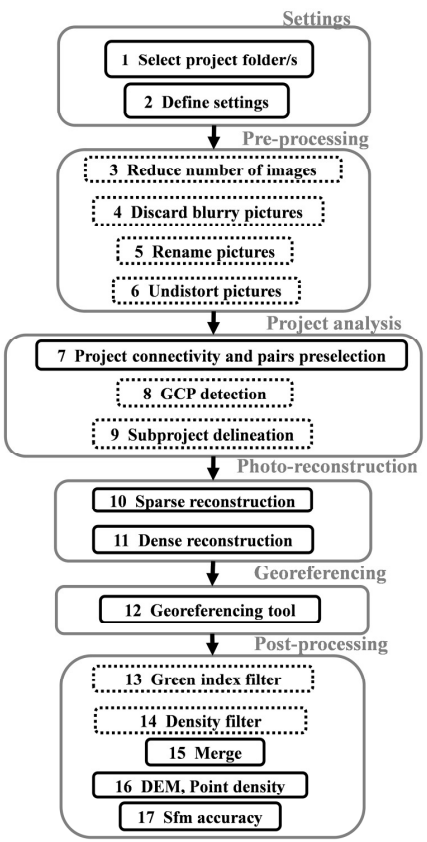
Settings
1 Select project folder/s
2 Define settings
Pre-processing
3 Reduce number of images
4 Discard blurry pictures
5 Rename pictures
6 Undistort pictures
Project analysis
7 Project connectivity and pairs preselection
8 GCP detection
9 Subproject delineation
Photo-reconstruction
10 Sparse reconstruction
11 Dense reconstruction
Georeferencing
12 Georeferencing tool
Post-processing
13 Green index filter
14 Density filter
15 Merge
16 DEM, Point density
17 Sfm accuracy

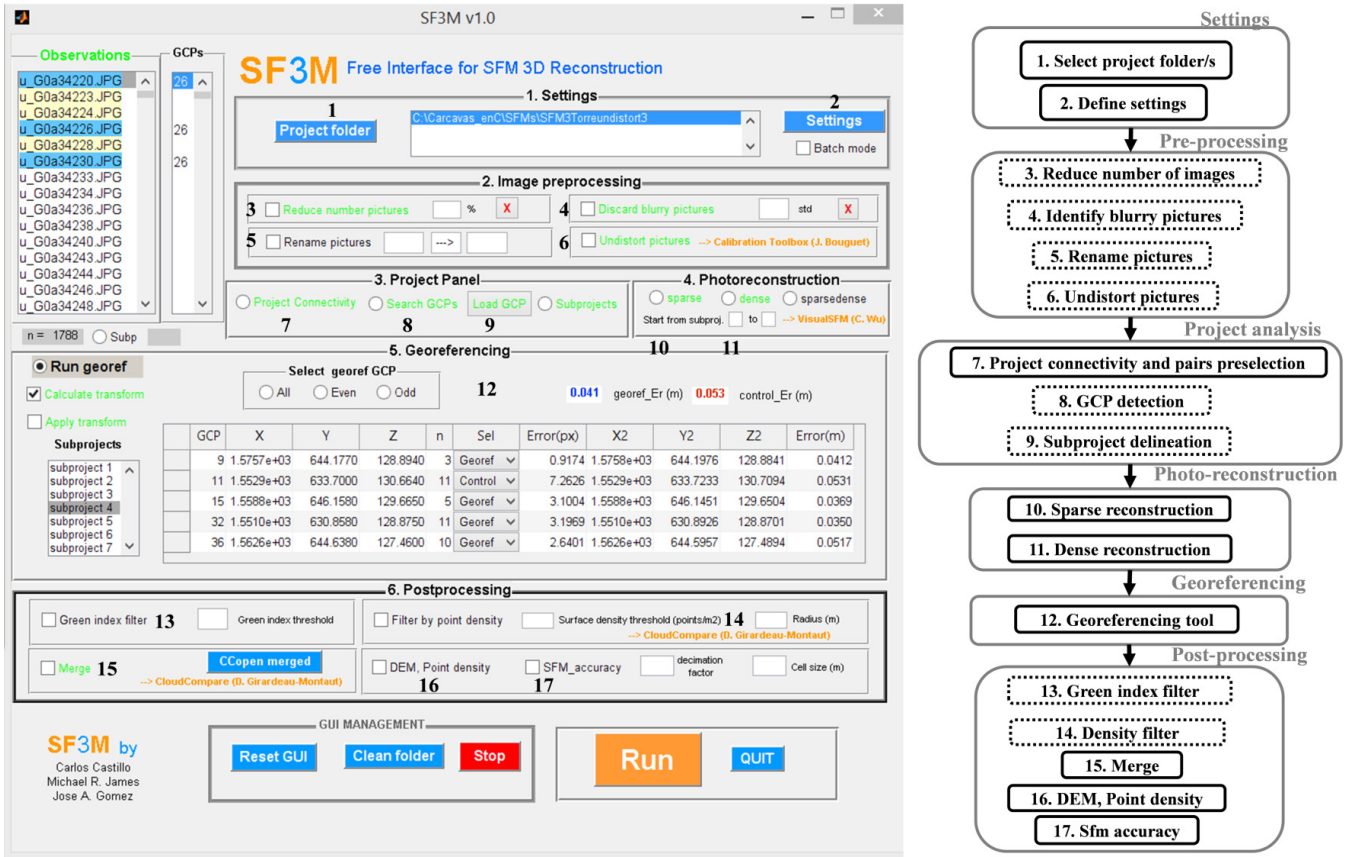

Figure 4. SF3M v1.0 workflow stages and their correspondence with command options on the SF3M main window. The dotted lines in the diagram indicate optional stages in a reconstruction project.

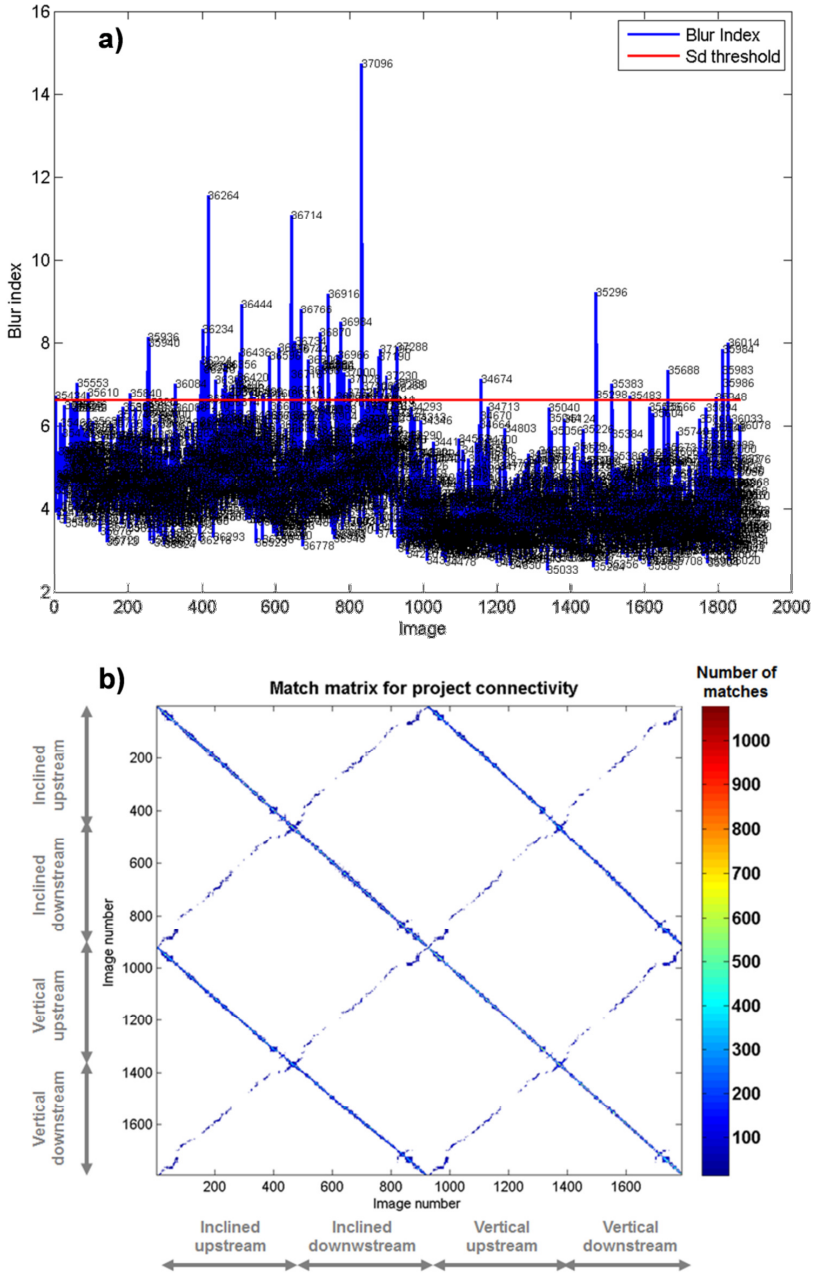

611

612 Figure 5. SF3M results of the pre-processing and project analysis stages for the gully
613 branch 2: a) Blur index for the ~1800 image set with image number label. Those images
614 outside the upper 2 standard deviations interval (red line) were discarded; b) matrix of
615 matches with indication of the camera and direction in the image collection (in grey).
616 The matrix of matches is symmetrical. Matches in the diagonal correspond to image sets
617 only connected in the linear direction.

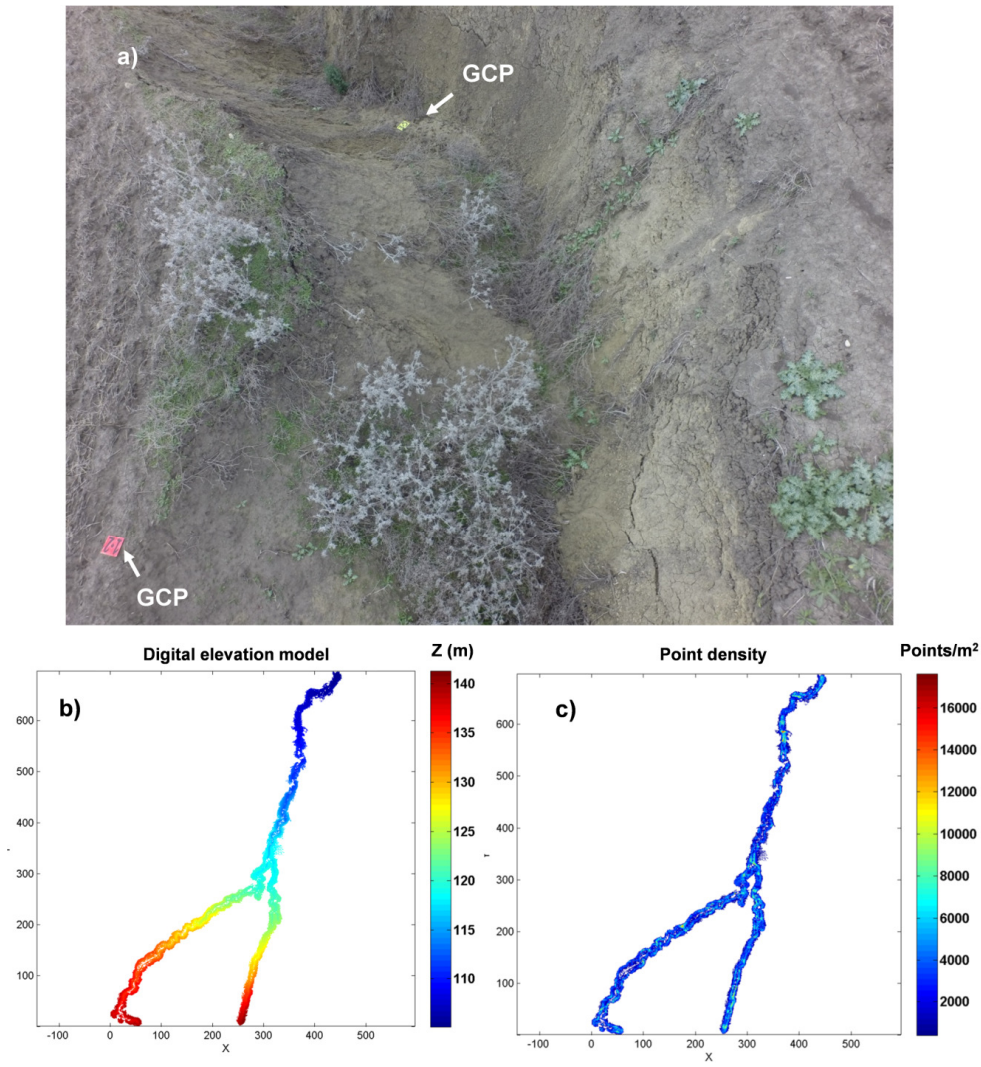

Figure 6. a) View of gully branch 2 from the inclined camera showing two ground control points GCPs; b) Digital elevation model (m) and c) point density map (points/m^2) for the entire gully network from SF3M results. Several gaps in the 3D model can be noticed as a result of vegetation occlusion, mainly small green weeds (removed by the green index filter) and tall grey weeds (filtered by applying the point classification by CANUPO).

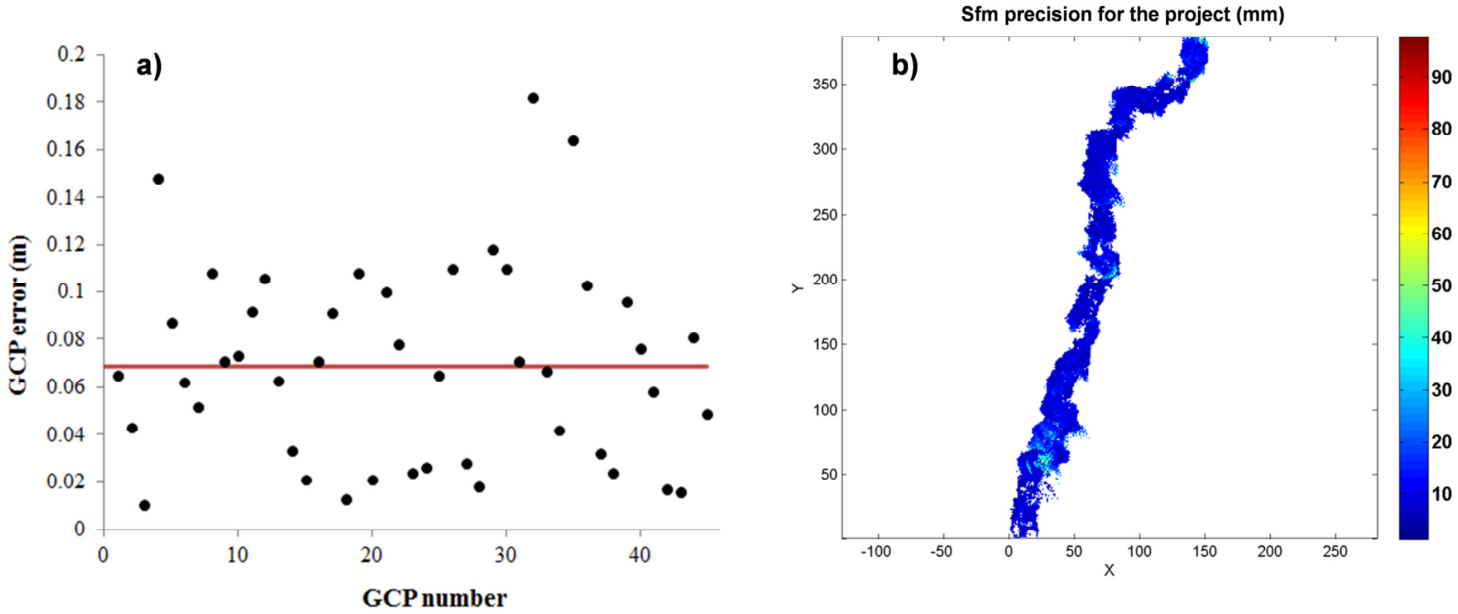

625

626 Figure 7. a) Error magnitudes on the 3D model (m) with dGPS ground control point measurements as the reference (the 0.069 m average in red
627 line); b) Estimated SfM local precision in mm (Eq. 1) taking into account the residuals in the image measurements and the camera-point distance
628 for gully branch 1. The dominant dark blue colours show that average precision is around 1-2 cm.

629

630

631

Figure 8. Views of the gully network in the 2007, 2009 and 2011 orthophotographies (Junta de Andalucía, 2015). Most probably, the gully was landfilled in the summer of 2008 and, since then, there is no evidence of having been filled again.